

N-donor-stabilized Pd(II) species supported by sulphonamide-azo ligands: Ligand architecture, solvent co-ligands, C–C coupling

Hammed Olawale Oloyede ^{a, b}, Joseph Anthony Orighomisan Woods ^a, Helmar Görls ^b, Winfried Plass ^{b, **}, Abiodun Omokehinde Eseola ^{b, c, *}

^a Inorganic Chemistry Unit, Department of Chemistry, University of Ibadan, Ibadan, Nigeria

^b Institut für Anorganische und Analytische Chemie, Friedrich-Schiller-Universität Jena, Humboldtstraße 8, 07743, Jena, Germany

^c Materials Chemistry Group, Department of Chemical Sciences, Redeemer's University Ede, Osun State, Nigeria

ARTICLE INFO

Article history:

Received 18 June 2019

Received in revised form

9 August 2019

Accepted 2 September 2019

Available online xxx

Keywords:

Catalyst design

Ligand effects

Suzuki-Miyaura

Heck-Mizoroki

Homogeneous catalysis

C–C coupling

ABSTRACT

In this report, a series of synthetically affordable phosphine-free ligands (**L1** – **L4**) of the form $\text{RSO}_2\text{--NH--Ph--N=N--Ph--NH--SO}_2\text{R}$ were prepared and examined as organic ligands for stabilizing palladium active centers; R = methyl, tolyl or triisopropylphenyl. Palladium complexes, which were obtained in varying coordination environments as well as with varying complementary co-ligands (water, acetonitrile or pyridine), have been subjected to Suzuki and Heck coupling experiments in order to study molecular level ligand effects on preferred catalyst settings. The appreciable coupling activities for Suzuki and Heck coupling with functional group tolerance were recorded for palladium species generated from the chelate ligands. Results show that, despite the tridentate chelation characteristics of these azo-benzene ligands, the introduction of bulky units at the sulfonyl groups enabled generation of active palladium species with high turnover frequencies; e.g. 5040 h^{-1} (84% yield) within 5 min at 0.2 mol % loading of **Pd.L2.py** in only water as solvent. A correlation between catalytic efficiencies and the bulkiness of the coordinated co-ligand was obtained. However, while Suzuki coupling activity increased with increase in co-ligand sizes of the preformed complexes (i.e. water < acetonitrile < pyridine), the pyridyl co-ligand turned out to be very unfavourable for Heck coupling where the acetonitrile-complemented complexes possessed the higher activities. Therefore, it could be concluded that the best catalyst setting for Suzuki coupling may not be the best for Heck reaction.

© 2019 Elsevier B.V. All rights reserved.

1. Introduction

Palladium-catalyzed cross couplings of organic substrates has become a dominant synthetic tool in many industrial and academic fields associated with routine organic chemistry syntheses [1–16]. The joint Nobel Prize award in chemistry to Suzuki, Heck and Negishi in 2010 highlights the importance of palladium-mediated cross coupling catalysis. Suzuki-Miyaura and Heck-Mizoroki coupling methods [17–20] remain the most frequently employed methods among the various carbon-coupling techniques [21–24].

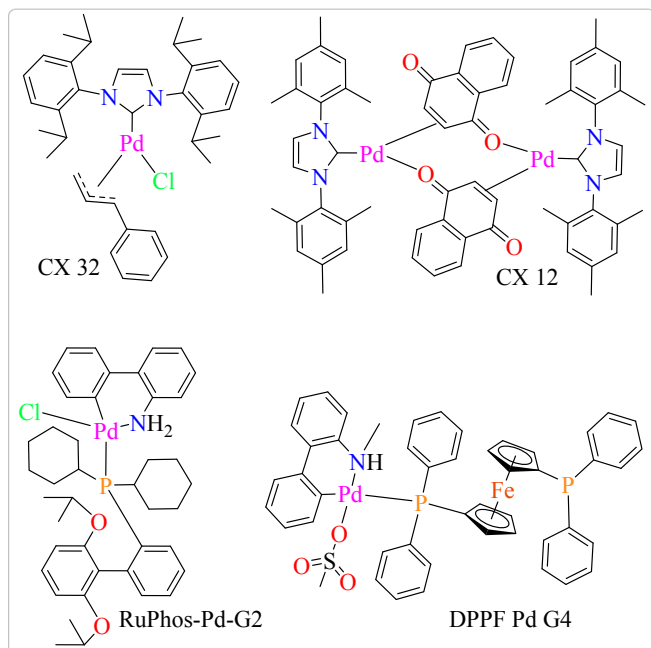
Although Suzuki-Miyaura reactions could be carried out under mild reaction conditions [25,26], Heck reactions are commonly performed at high temperatures, longer reaction durations, high catalyst loadings in the presence of promoters and, in some cases, under inert atmosphere [27–31].

Substantial efforts have been committed to the design and syntheses of palladium compounds as precatalysts for various research reasons [23,32] and with diverse ligand designs explored [33–36]. As a result, several highly active palladium pre-catalysts, which are often supported by N-heterocyclic carbene (NHC) and phosphine ligands [22,37–41] as well as imine-based ligands, have already been commercialized (Scheme 1) [40,42,43]. However, many of these NHC- and phosphine-based palladium complexes are commonly complemented by cyclometalating C^N or allylic organometallic co-ligands as well as halides [39]. In addition to being expensive, these commercialized precatalysts are confronted with air and moisture sensitivity problems [44]. Therefore,

* Corresponding author. Present Address: Institut für Anorganische und Analytische Chemie, Friedrich-Schiller-Universität Jena, Humboldtstr. 8, D-07743, Jena, Germany.

** Corresponding authors. Institut für Anorganische und Analytische Chemie, Friedrich-Schiller-Universität Jena, Humboldtstr. 8, D-07743, Jena, Germany.

E-mail addresses: sekr.plass@uni-jena.de (W. Plass), biodun.eseola@uni-jena.de, bioduneseola@hotmail.com (A.O. Eseola).



Scheme 1. Examples of highly active and commercially trademarked pre-catalysts.

exploring simpler and more stable N-donor pre-catalysts are considered necessary.

The rigidity and bulkiness with chelation characteristics of ligands are themes that have been associated with catalyst efficiencies in palladium-catalyzed C–C couplings [45–47]. Furthermore, the azo-benzenes containing the azo (–N=N–) functional group, which are characteristically photo-switchable between the *trans*- and *cis*-isomers [48–50], are hardly rarely seen in palladium coordination chemistries [51]. Consequently, alkyl/aryl-substituted sulfonyl groups have been used to functionalize 2,2'-(diazene-1,2-diyl)dianiline in this study [52–55].

We herein present the results of the synthesis, structural characterization and C–C coupling activities of palladium complexes based on structurally and electronically varied sulfonyl-substituted 2,2'-(diazene-1,2-diyl)dianiline ligands (**Scheme 2 (iii)**). *In situ* catalytic activity studies of the prepared ligands were also tested. In view of desires to promote green chemistry, couplings in water were mainly considered [19,39].

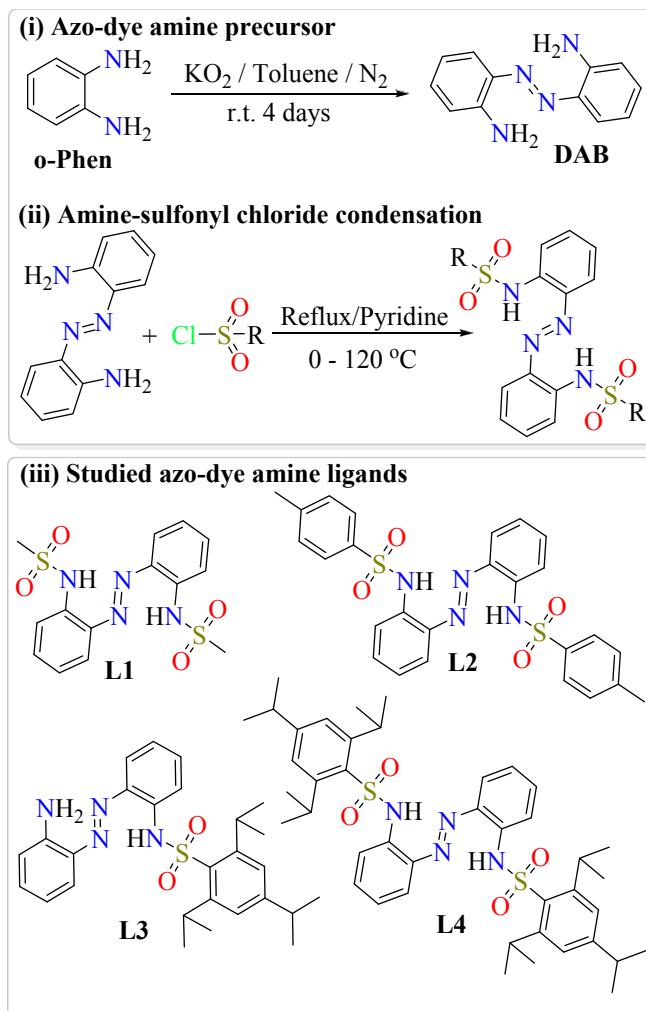
2. Experimental

2.1. General information

All starting materials for synthesis as well as substrates for the catalytic experiments were obtained commercially as reagent grade and used as supplied without further purification. Ligands and ligand intermediates were either purified on silica gel columns or recrystallized to exclude impurities. All air sensitive reactions were carried out under nitrogen inert atmosphere using a standard Schleck technique. IR spectra were measured with a Bruker Equinox FT-IR spectrometer equipped with a diamond ATR unit in the range of 4000–600 cm^{-1} . Elemental analyses were carried out on Leco CHNS-932 and El Vario III elemental analyzers. Mass spectrometry (MS) spectra were measured with a Bruker MAT SSQ 710 spectrometer. ^1H and ^{13}C NMR spectra were recorded with a Bruker AVANCE 400 MHz spectrometer.

2.2. Syntheses of the ligands

2,2'-Diaminoazobenzene (DAB): [56] *o*-Phenylenediamine (15.00 g, 138.8 mmol) and KO_2 chunks (15.00 g, 211.0 mmol) were weighed into a 1 L three-necked round-bottomed flask. The mixture was dissolved in dry toluene (650 mL) and stirred under nitrogen at room temperature. After two days, another 7.5 g of KO_2 chunks were carefully added and the reaction stirred for further 2 days. Although the reaction mixture still showed traces of the starting material, the remaining KO_2 was carefully quenched by slow addition of water (500 mL) followed by further stirring for additional 30 min. The organic layer was separated and the aqueous layer extracted using ethyl acetate (500 mL). The combined organic layers were washed with water (4 x 200 mL) and dried over MgSO_4 . The solution was concentrated under reduced pressure and the residue was purified by chromatography using silica gel and 1 n-hexane: 4 ethyl acetate mixture. The **DAB** was obtained as red crystals. Yield (5.1 g, 34%). Selected IR data (ATR, cm^{-1}): ν 3458m, 3354m, 3057w, 1599s, 1573s, 1476s, 1455s, 1304s, 1254s, 1136s, 739vs. ^1H NMR (400 MHz, $\text{DMSO}-d_6$): δ_{ppm} 7.66 (d, $J = 8.1$ Hz, 2H), 7.13 (dd, $J = 11.1, 4.0$ Hz, 2H), 6.85 (d, $J = 8.1$ Hz, 2H), 6.61 (t, $J = 7.5$ Hz, 2H), 6.38 (s, 4H). ^{13}C NMR (101 MHz, $\text{DMSO}-d_6$): δ 145.70, 137.15, 131.69, 122.33, 117.21, 116.11. MS (EI) m/z 212 (M^+ , 100%); 183, 169, 120, 92, 65. Anal. Calc. for $\text{C}_{12}\text{H}_{12}\text{N}_4$: C, 67.90; H, 5.70; N,



Scheme 2. (i – ii) Synthetic schemes and (iii) products of synthesized chelating ligands.

26.40%. Found: C, 67.79; H, 5.69; N, 26.38%.

(E)-N,N'-(diazene-1,2-diylbis(2,1-phenylene))dimethanesulfonamide (L1): Methanesulfonyl chloride (1.37 mL, 17.67 mmol) was added dropwise to a solution of **DAB** (1.25 g, 5.89 mmol) in 20 mL of pyridine at 0 °C while stirring in a 50 mL round-bottomed flask. The reaction mixture was then stirred at room temperature for 12 h and subsequently concentrated under reduced pressure. Ethanol (5 mL) was added to the residue, filtered and washed with chloroform (5 mL) followed by ethanol (10 mL). **L1** was obtained as a yellow powder. Yield (1.83 g, 84%). Mp = 264 °C. Selected IR data (ATR cm^{-1}): ν 3458m, 3360m, 3057w, 3025w, 1598s, 1570s, 1476m, 1304s, 1217s, 1137s, 739vs. ^1H NMR (400 MHz, DMSO- d_6): δ_{ppm} 9.83 (s, 2H), 8.00 (d, $J = 8.0$ Hz, 2H), 7.60 (dt, $J = 15.2, 7.7$ Hz, 4H), 7.35 (t, $J = 7.2$ Hz, 2H), 3.08 (s, 6H). ^{13}C NMR (101 MHz, DMSO- d_6): δ 143.97, 137.27, 133.22, 125.57, 124.19, 118.02, 55.36. MS (EI) m/z 368 (M^+ , 45%); 289, 210, 198, 181, 154, 108, 91, 79, 65, 51. Anal. Calc. for $\text{C}_{14}\text{H}_{16}\text{N}_4\text{O}_4\text{S}_2$: C, 45.64; H, 4.38; N, 15.21; S, 17.41%. Found: C, 45.58; H, 4.42; N, 14.96; S, 17.76%.

(E)-N,N'-(diazene-1,2-diylbis(2,1-phenylene))bis(4-methylbenzenesulfonamide) (L2): **DAB** (1.25 g, 5.89 mmol) and *p*-toluenesulfonyl chloride (3.37 g, 17.67 mmol) were mixed in 20 mL of pyridine inside a 50 mL round-bottom flask while stirring at room temperature. The reaction mixture was then refluxed at 100 °C for 12 h. The product was concentrated under reduced pressure. Ethanol (5 mL) was added to the residue which was filtered and then washed with chloroform (5 mL) and ethanol (10 mL) to give **L2** as an orange powder. Yield (2.82 g, 92%). Mp = 272 °C. Selected IR data (ATR cm^{-1}): ν 3265m, 3251m, 3085w, 1594s, 1481s, 1386s, 1332s, 1161vs, 1089vs, 904vs, 654vs. ^1H NMR (400 MHz, DMSO- d_6): δ_{ppm} 10.17 (s, 2H), 7.67–7.54 (m, 6H), 7.51 (d, $J = 3.9$ Hz, 4H), 7.26 (dt, $J = 8.3, 4.2$ Hz, 2H), 7.14 (d, $J = 8.0$ Hz, 4H), 2.18 (s, 6H). ^{13}C NMR (101 MHz, DMSO- d_6): δ_{ppm} 144.19, 143.59, 137.44, 136.57, 132.85, 129.86, 127.06, 125.72, 125.09, 117.75, 21.28. MS (EI) m/z 520 (M^+ , 98%); 365, 347, 210. Anal. Calc. for $\text{C}_{26}\text{H}_{24}\text{N}_4\text{O}_4\text{S}_2$: C, 59.98; H, 4.65; N, 10.76; S, 12.32%. Found: C, 60.13; H, 4.66; N, 10.79; S, 12.45%.

(E)-N-(2-((2-aminophenyl)diazanyl)phenyl)-2,4,6-triisopropylbenzenesulfonamide (L3) and **(E)-N,N'-(diazene-1,2-diylbis(2,1-phenylene))bis(2,4,6-triisopropylbenzenesulfonamide) (L4):** 2, 4, 6-triisopropylbenzenesulfonyl chloride, (3.57 g, 11.78 mmol) was added to a pyridine (20 mL) solution of **DAB** (1.25 g, 5.89 mmol) in a 50 mL round-bottom flask. The reaction mixture was refluxed at 120 °C for 12 h. The mixture was concentrated under reduced pressure to obtain the crude product. Purification was carried out on column chromatography with silica gel, *n*-hexane/THF (7:3) and later chloroform/methanol (1:1). **L3** was obtained as a red powder while yellow powder of **L4** was eluted as the second product.

L3: Yield (1.20 g, 28%). Mp = 249 °C. Selected IR data (ATR cm^{-1}): ν 3449m, 3290w, 2959s, 2867w, 1617s, 1599s, 1556s, 1482s, 1307s, 1226s, 1149vs, 1039vs, 908s, 753 vs, 651vs. ^1H NMR (400 MHz, DMSO- d_6): δ_{ppm} 10.28 (s, 1H), 7.82–7.71 (m, 1H), 7.62–7.47 (m, 1H), 7.34 (t, $J = 7.1$ Hz, 1H), 7.30–7.23 (m, 2H), 7.19 (s, 3H), 6.89 (s, 2H), 6.85 (d, $J = 8.1$ Hz, 1H), 6.58 (t, $J = 7.2$ Hz, 1H), 4.06 (dt, $J = 13.3, 6.6$ Hz, 2H), 2.99–2.75 (m, 1H), 1.17 (d, $J = 6.9$ Hz, 6H), 1.08 (d, $J = 6.7$ Hz, 12H). ^{13}C NMR (101 MHz, DMSO- d_6): δ 152.90, 151.45, 150.28, 146.11, 145.24, 137.58, 136.53, 134.47, 134.14, 133.38, 132.48, 130.74, 126.07, 125.19, 124.27, 124.18, 118.97, 117.41, 115.77, 79.64, 33.72, 29.65, 25.03, 23.80. MS (EI) m/z 478 (M^+ , 60%); 371, 357, 293, 211, 183, 120, 91. Anal. Calc. for $\text{C}_{27}\text{H}_{34}\text{N}_4\text{O}_2\text{S}_2$: C, 67.75; H, 7.16; N, 11.71; S, 6.70%. Found: C, 67.79; H, 7.11; N, 11.72; S, 6.34%.

L4: Yield (1.45 g, 33%). Mp = 158 °C. Selected IR data (ATR cm^{-1}): ν 3290s, 2960s, 2871m, 1591m, 1558m, 1479s, 1378s, 1281 vs, 1165vs, 1150vs, 1039s, 906vs, 825s, 665vs. ^1H NMR (400 MHz, d_6 - CDCl_3): δ_{ppm} 10.07 (s, 2H), 7.63 (d, $J = 7.8$ Hz, 2H), 7.47 (d,

$J = 8.3$ Hz, 2H), 7.36 (t, $J = 7.6$ Hz, 2H), 7.17 (s, 2H), 7.12 (t, $J = 7.6$ Hz, 2H), 4.31 (hept, $J = 6.7$ Hz, 4H), 2.90 (dt, $J = 13.8, 6.9$ Hz, 2H), 1.25 (d, $J = 6.9$ Hz, 12H), 1.21 (d, $J = 6.7$ Hz, 24H). ^{13}C NMR (101 MHz, d_6 - CDCl_3): δ 153.53, 150.66, 137.89, 135.44, 133.05, 132.28, 124.13, 123.10, 122.93, 117.68, 34.12, 29.81, 25.61, 24.74, 23.47. MS (EI) m/z 744 (M^+ , 40%); 477, 371, 267. Anal. Calc. for $\text{C}_{42}\text{H}_{56}\text{N}_4\text{O}_4\text{S}_2$: C, 66.90; H, 7.62; N, 7.43; S, 8.50%. Found: C, 67.16; H, 7.53; N, 7.50; S, 8.32%.

2.3. Syntheses of palladium complexes

Pd.L1.w: **L1** (30 mg, 0.08 mmol) and palladium(II) acetate (18 mg, 0.08 mmol) were added together in chloroform (2 mL). The clear solution was then precipitated by addition of *n*-hexane to obtain **Pd.L1.w** as brown powder. Yield (20 mg, 51%). Mp = 299 °C. Selected IR data (ATR cm^{-1}): ν 3380w (br), 3043w, 1590m, 1572w, 1543w, 1475m, 1292vs, 1220vs, 1162m, 1119vs, 954vs, 844vs, 761vs, 627vs. MS (EI) m/z 490 (M^+ , 7%), 494 ($\text{M}^+ - \text{H}_2\text{O} + \text{Na}$), (473 ($\text{M}^+ - \text{H}_2\text{O}$, 20%), 391 ($\text{L}^+ + \text{Na}$). Anal. Calc. for $\text{C}_{14}\text{H}_{16}\text{N}_4\text{O}_5\text{PdS}_2 \cdot \text{H}_2\text{O} \cdot \frac{1}{2}\text{CH}_3\text{COOH}$: C, 33.43; H, 3.74; N, 10.40; S, 11.90%. Found: C, 33.26; H, 3.34; N, 10.17; S, 11.64%.

Pd.L1.acn: **L1** (30 mg, 0.08 mmol) and palladium(II) acetate (18 mg, 0.08 mmol) were added together and dissolved in acetonitrile (1 mL) layered with diethylether (1 mL). The clear solution was allowed to stand for 1 day. The microcrystalline product was filtered, washed with acetonitrile and air-dried to give **Pd.L1.acn** as a purple solid. Yield (0.03 g, 74%). Mp = 293–295 °C. Selected IR data (ATR cm^{-1}): ν 2347w, 2309w, 1593m, 1570m, 1453m, 1292vs, 1118vs, 952vs, 837vs, 746vs, 626vs. MS (EI) m/z 473 ($\text{M}^+ - \text{CH}_3\text{CN}$, 20%); 392, 314, 288, 212, 176, 105, 79, 41, 28. Anal. Calc. for $\text{C}_{16}\text{H}_{17}\text{N}_5\text{O}_4\text{PdS}_2 \cdot \text{C}_3\text{H}_7\text{N}$: C, 37.40; H, 3.33; N, 13.63; S, 12.48%. Found: C, 37.79; H, 3.27; N, 13.60; S, 12.52%.

Pd.L1.py: **L1** (30 mg, 0.08 mmol), palladium(II) acetate (18 mg, 0.08 mmol) and pyridine (0.1 mL) were added together in acetonitrile (2 mL). **Pd.L1.py** was obtained as purple powder the following day. Yield (0.04 g, 90%). Mp = 220 °C. Selected IR data (ATR cm^{-1}): ν 2945w, 2877w, 1590m, 1451s, 1295vs, 1239m, 1125vs, 945vs, 856vs, 753vs, 695vs. MS (EI) m/z 474 ($\text{M}^+ - \text{Py}$, 20%), 368 (L^+ , 15%), 289, 210, 108, 79 (Py^+), 52, 28. Anal. Calc. for $\text{C}_{19}\text{H}_{19}\text{N}_5\text{O}_4\text{PdS}_2 \cdot 1.3\text{CH}_3\text{CN}$: C, 42.86; H, 3.81; N, 14.58; S, 10.59%. Found: C, 43.27; H, 3.65; N, 14.21; S, 10.45%.

Pd.L2: **L2** (30 mg, 0.06 mmol) and palladium(II) acetate (13 mg, 0.06 mmol) were added together and dissolved in chloroform (1 mL). The clear solution was layered with *n*-hexane to give **Pd.L2** as purple crystals. Single crystal suitable for X-ray measurement was obtained from the mother liquor. Yield (0.02 g, 54%). Mp = 325–327 °C. Selected IR data (ATR cm^{-1}): ν 1690m, 1590m,

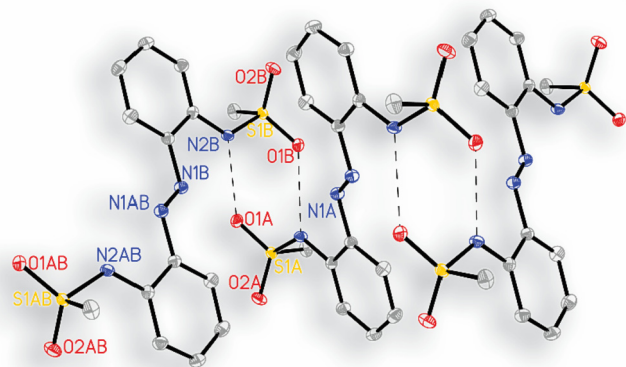
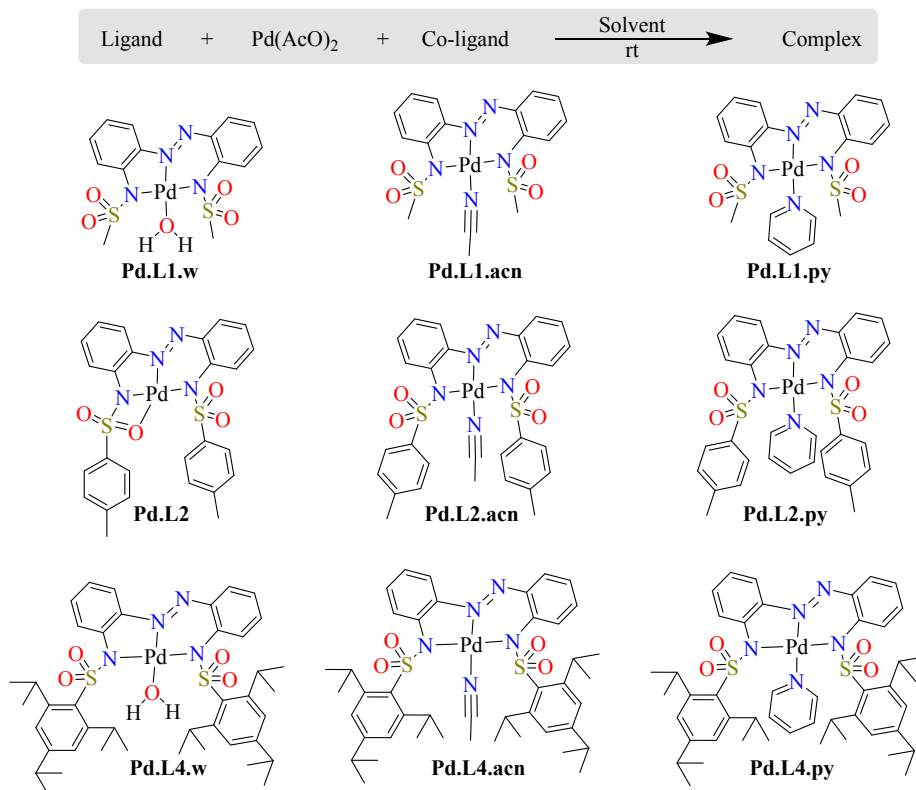


Fig. 1. Ortep plot of ligand **L1** with thermal ellipsoids drawn at the 40% probability level. Protons have been omitted for clarity.



1546m, 1421m, 1304s, 1228s, 1140s, 1079s, 939s, 658vs. MS (ESI) m/z 625 (M^+ , 100%): 646 ($[M^+ + Na]$, 100%). Anal. Calc. for $C_{26}H_{22}N_4O_4PdS_2$: C, 49.96; H, 3.55; N, 8.96; S, 10.26%. Found: C, 49.98; H, 3.48; N, 9.00; S, 10.37%.

Pd.L2.acn: **L2** (30 mg, 0.06 mmol) and palladium(II) acetate (13 mg, 0.06 mmol) were added together and dissolved in acetonitrile (1 mL). The clear solution was layered with diethylether (1 mL) and allowed to stand for 3 days. **Pd.L2.acn** was obtained as

Table 1
Crystal data and refinement details for the X-ray structure determinations of the ligand **L1** and complexes **Pd.L2** – **Pd.L4.py**.

Compound	L1	Pd.L2	Pd.L2.acn	Pd.L2.py	Pd.L4.acn	Pd.L4.py
formula	$C_{14}H_{16}N_4O_4S_2$	$C_{26}H_{22}N_4O_4PdS_2$	$C_{28}H_{25}N_5O_4PdS_2$	$C_{31}H_{27}N_5O_4PdS_2$	$C_{44}H_{57}N_5O_4PdS_2$ [*]	$C_{47}H_{59}N_5O_4PdS_2$ [*]
fw ($g \cdot mol^{-1}$)	368.43	625.00	666.05	704.10	890.46[*]	928.51[*]
$^{\circ}C$	-140(2)	-140(2)	-140(2)	-140(2)	-140(2)	-140(2)
crystal system	orthorhombic	Triclinic	triclinic	monoclinic	monoclinic	monoclinic
space group	P b c n	P $\bar{1}$	P $\bar{1}$	P 2 ₁ /c	P 2 ₁ /c	P 2 ₁ /c
a/ \AA	21.2115(6)	8.9570(2)	8.7606(6)	17.1098(4)	17.6369(4)	17.6300(2)
b/ \AA	7.8440(2)	13.1679(3)	12.2968(9)	8.1173(2)	16.4686(4)	17.2122(3)
c/ \AA	9.6694(2)	21.3330(3)	14.1200(10)	22.6646(5)	17.0233(4)	17.2556(3)
$\alpha/^\circ$	90	93.815(1)	68.308(2)	90	90	90
$\beta/^\circ$	90	97.185(1)	74.082(2)	107.378(1)	112.460(1)	113.666(1)
$\gamma/^\circ$	90	99.427(1)	78.832(2)	90	90	90
$V/\text{\AA}^3$	1608.82(7)	2452.89(9)	1351.92(17)	3004.10(12)	4569.44(19)	4795.87(13)
Z	4	4	2	4	4	4
ρ ($g \cdot cm^{-3}$)	1.521	1.692	1.636	1.557	1.294	1.286
μ (cm^{-1})	3.59	9.69	8.86	8.02	5.42[*]	5.21[*]
measured data	11602	32585	13659	20467	55905	35477
data with $I > 2\sigma(I)$	1654	9762	4568	6366	8309	9301
unique data (R_{int})	1829/0.0393	11194/0.0293	5262/0.0300	6827/0.0437	10451/0.0616	10947/0.0536
wR_2 (all data, on F^2) ^{a)}	0.0784	0.0766	0.1307	0.0906	0.1292	0.1065
R_1 ($I > 2\sigma(I)$) ^{a)}	0.0317	0.0355	0.0478	0.0453	0.0664	0.0515
S ^{b)}	1.087	1.054	1.054	1.182	1.167	1.115
Res. dens./ $e \cdot \text{\AA}^{-3}$	0.332/-0.359	0.923/-0.666	0.651/-0.743	0.688/-0.835	1.018/-0.863	1.106/-0.624
absorpt method	multi-scan	multi-scan	multi-scan	multi-scan	multi-scan	multi-scan
absorpt corr T_{min}/max	0.7048/0.7456	0.7043/0.7456	0.5884/0.7456	0.6641/0.7456	0.6798/0.7456	0.7102/0.7456
CCDC No.	1880299	1880300	1880301	1880302	1880303	1880304

* Derived parameters do not contain the contribution of the disordered solvent.

^{a)} Definition of the R indices: $R_1 = (\sum ||F_o| - |F_c||) / \sum |F_o|$; $wR_2 = [\sum [w(F_o^2 - F_c^2)^2] / \sum [w(F_o^2)^2]]^{1/2}$ with $w^{-1} = \sigma^2(F_o^2) + (aP)^2 + bP$; $P = [2F_c^2 + \text{Max}(F_o^2)]/3$.

^{b)} $S = [\sum [w(F_o^2 - F_c^2)^2] / (N_o - N_p)]^{1/2}$.

purple crystals from which single crystal was picked for X-ray measurement. Yield (0.03 g, 75%). Mp = 316 °C. Selected IR data (ATR cm^{-1}): ν 2936w, 2325w, 1674m, 1594m, 1546m, 1418m, 1309m, 1229s, 1142vs, 1081vs, 912vs, 860vs, 751vs, 657vs. MS (EI) m/z 625 ($M^+ - \text{CH}_3\text{CN}$, 100%): 558, 467, 406, 366, 41. Anal. Calc. for $\text{C}_{28}\text{H}_{25}\text{N}_5\text{O}_4\text{PdS}_2$: C, 50.49; H, 3.78; N, 10.51; S, 9.63%. Found: C, 50.77; H, 3.70; N, 10.55; S, 9.56%.

Pd.L2.py: **L2** (30 mg, 0.06 mmol), palladium(II) acetate (13 mg, 0.06 mmol) and pyridine (0.1 mL) were added together and dissolved in acetonitrile (1 mL). The clear solution was allowed to stand for 1 week under slow evaporation after which crystals suitable for X-ray measurement were obtained. Yield (0.03 g, 67%). Mp = 273 °C. Selected IR data (ATR cm^{-1}): ν 1609m, 1588m, 1466m, 1214m, 1140vs, 1082vs, 910vs, 838vs, 755vs, 663vs. MS (EI) m/z 624 ($[M^+ - \text{Py}]$, 7%): 646 ($[M^+ - \text{Py} + \text{Na}]$, 100%). Anal. Calc. for

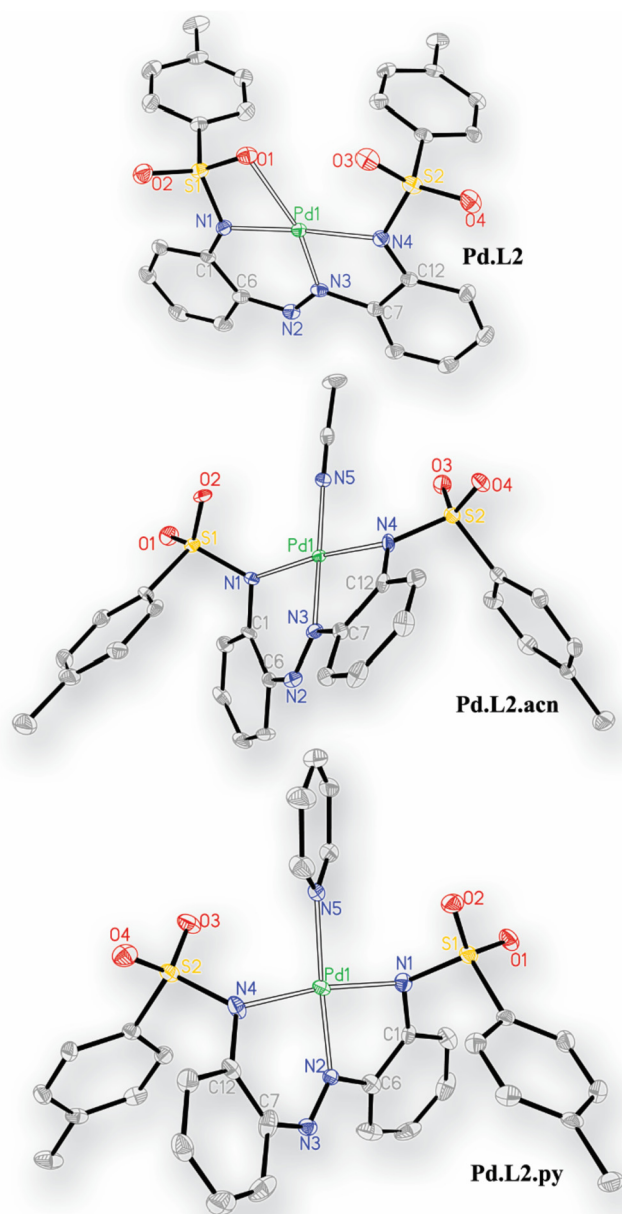


Fig. 2. Ortep plots of complexes **Pd.L2**, **Pd.L2.acn** and **Pd.L2.py** with thermal ellipsoids drawn at the 40% probability level. Protons have been omitted for clarity.

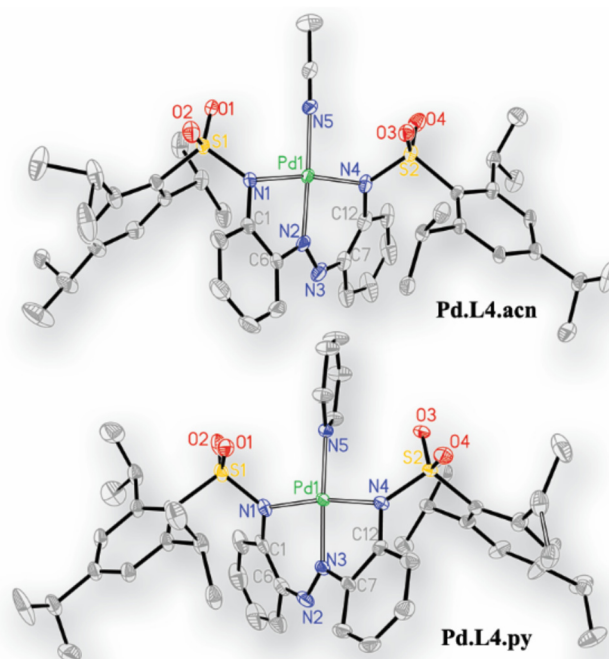


Fig. 3. Ortep plots of palladium complexes **Pd.L4.acn** and **Pd.L4.py** with thermal ellipsoids drawn at the 40% probability level. Protons have been omitted for clarity.

$\text{C}_{31}\text{H}_{27}\text{N}_5\text{O}_4\text{PdS}_2$: C, 52.88; H, 3.87; N, 9.95; S, 9.11%. Found: C, 52.67; H, 3.76; N, 10.10; S, 8.98%.

Pd.L4.w: **L4** (30 mg, 0.04 mmol) and palladium(II) acetate (9 mg, 0.04 mmol) were added together and dissolved in chloroform (2 mL). The clear solution was layered with n-hexane. After 1 day, the crystalline product was filtered, washed with hexane and air-dried to give **Pd.L4.w** as a purple solid. Yield (30 mg, 86%). Mp = 210 °C. Selected IR data (ATR cm^{-1}): ν 3317w (br), 2951m, 2863w, 1600m, 1538w, 1475m, 1415m, 1301m, 1214s, 1119vs, 1031vs, 942vs, 819vs/745vs, 629vs. MS (EI) m/z 848 ($M^+ - \text{H}_2\text{O}$, 25%): 837, 778, 720, 671, 614, 553, 512, 447, 386, 332, 272. Anal. Calc. for $\text{C}_{42}\text{H}_{56}\text{N}_4\text{O}_5\text{PdS}_2 \cdot \text{H}_2\text{O}$: C, 56.97; H, 6.60; N, 6.33; S, 7.24%. Found: C, 57.25; H, 6.45; N, 6.23; S, 7.07%.

Pd.L4.acn: **L4** (30 mg, 0.04 mmol) and palladium(II) acetate (9 mg, 0.04 mmol) were added together and dissolved in acetonitrile (2 mL). The clear solution was allowed to stand for 3 days under slow evaporation to obtain purple crystals suitable for X-ray measurement. Yield (30 g, 81%). Mp = 198 °C. Selected IR data (ATR cm^{-1}): ν 2956m, 2863w, 2312w, 1599m, 1544m, 1420s, 1295s, 1234m, 1131m, 1033vs, 941m, 845vs, 757vs, 649vs. MS (ESI) m/z 873 ($[M^+ - \text{CH}_3\text{CN}]$), 100%. Anal. Calc. for $\text{C}_{44}\text{H}_{57}\text{N}_5\text{O}_4\text{PdS}_2$: C, 59.35; H, 6.45; N, 7.86; S, 7.20%. Found: C, 59.35; H, 6.41; N, 7.79; S, 7.13%.

Pd.L4.py: **L4** (30 mg, 0.04 mmol), palladium(II) acetate (9 mg,

Table 2

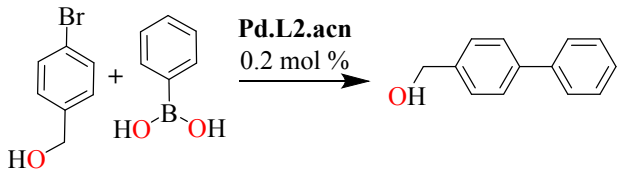
Selected bond lengths (Å) around the metal centers of **Pd.L2**, **Pd.L2.acn**, **Pd.L2.py**, **Pd.L4.acn** and **Pd.L4.py**

Bonds lengths (Å)	Pd.L2	Pd.L2.acn	Pd.L2.py	Pd.L4.acn	Pd.L4.py
Pd1–N1	1.960(2)	2.006(4)	2.037(3)	2.041(3)	2.013(3)
Pd1–N2/Pd1–N3 ^a	1.927(2)	1.945(4)	1.978(3)	1.958(4)	1.957(3)
Pd1–N4	2.023(2)	2.041(4)	2.018(3)	2.026(3)	2.052(3)
Pd1–N5/Pd1–O1	2.257(2) ^b	2.022(4)	2.034(3)	2.017(4)	2.033(3)

^a Pertains to N-azo bonds with the palladium(II) center.

^b Pd–O bond.

Table 3
Optimization of reaction parameters for Suzuki-Miyaura coupling



Entry	Complex (solvent)	Time (min)	Base	Yield (%) ^a
1	Pd.L2.acn (EtOH/H ₂ O)	10	K ₃ PO ₄	83
3	Pd.L2.acn (EtOH/H ₂ O)	10	K ₂ CO ₃	93
6	Pd.L2.acn (H ₂ O)	10	K ₂ CO ₃	92

Reaction conditions: Solvent (4 mL), base (1.0 mmol), time (30 min reflux), temperature of oil bath (100 °C), Pd-catalyst (0.2 mol%), (4-bromophenyl)methanol (1.0 mmol), benzeneboronic acid (1.2 mmol).

^a Yield was determined by ¹H NMR and reported to the nearest whole number.

0.04 mmol) and pyridine (0.2 mL) were allowed to stand in acetonitrile (1 mL) to obtain **Pd.L4.py** as purple crystals after 2 days. Yield (0.027 g, 73%). Mp = 283–285 °C. Selected IR data (ATR cm⁻¹): ν 3049w, 2945s, 2858m, 1599s, 1453s, 1360m, 1293s, 1238s, 1139vs, 1071s, 841vs, 837vs, 754vs, 649vs. MS (ESI) *m/z* 849 ([M⁺ - Py], 20%): 766 (L⁺ + Na), 743 (L⁺, 100%). Anal. Calc. for C₄₇H₅₉N₅O₄PdS₂: C, 60.79; H, 6.40; N, 7.54; S, 6.91%. Found: C, 60.92; H, 6.36; N, 7.82; S, 6.53%.

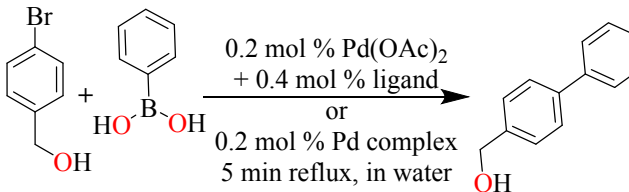
2.4. Suzuki-Miyaura coupling experiment

In a typical catalytic reaction, (4-bromophenyl)methanol (0.19 g, 1.0 mmol), benzeneboronic acid (0.15 g, 1.2 mmol), K₃CO₃ (0.14 g, 1.0 mmol) and preformed complex (0.2 mol % relative to (4-bromophenyl)methanol) were added together in a 10 mL round-bottom flask equipped with magnetic stirrer bar. In the case of *in situ*, 0.2 mol % Pd(OAc)₂ and 0.4 mol % ligand were used relative to (4-bromophenyl)methanol. Water (4 mL) was added and the mixture refluxed on an oil bath set at 100 °C for the desired reaction time. An aliquot of the reaction mixture was taken into a 10 mL conical flask which was dried under vacuum to exclude the solvents. The residue was subjected to ¹H NMR measurement using deuterated DMSO. The reactivity of the catalyst was evaluated by comparison of the NMR signals for the methylene (-CH₂-) protons of (4-bromophenyl)methanol at δ ≈ 4.4 ppm with that of the corresponding biphenyl product at δ ≈ 4.6 ppm. The yields were estimated by determining the integral of the product peak as a percentage of the sum of all observed methylene signals [57].

2.5. Heck coupling catalysis experiment

For typical Heck reaction, (4-bromophenyl)methanol (0.19 g, 1.0 mmol), styrene (0.17 mL, 1.5 mmol), K₂CO₃ (0.17 g, 1.5 mmol) and preformed complex (0.2 mol % relative to (4-bromophenyl)methanol) were added together in a 10 mL round-bottom flask equipped with magnetic stirrer bar. DMF (3 mL) and water (1 mL) were added and the mixture refluxed on an oil bath set at 140 °C for the desired reaction time. An aliquot of the reaction mixture was taken directly into NMR tube with deuterated DMSO and subjected to ¹H NMR. The reactivity of the catalyst was evaluated by comparison of the NMR signals observed for the methylene (-CH₂-) protons of (4-bromophenyl)methanol and (4-vinylphenyl)methanol at δ ≈ 4.4 ppm with that of the corresponding Heck product at δ ≈ 4.6 ppm. The yields were estimated by determining the integral of the product peak as a percentage of the sum of all observed

Table 4
Catalytic performance of the prepared palladium complexes



Catalyst	Temp (°C)	Yield (%)	TOF (h ⁻¹)
L1 + Pd(OAc) ₂	100	5	300
L2 + Pd(OAc) ₂	100	23	1380
L3 + Pd(OAc) ₂	100	46	2760
L4 + Pd(OAc) ₂	100	63	3780
Pd(OAc) ₂ alone	100	56	3360
Pd.L1.w	100	3	180
Pd.L1.acn	100	7	420
Pd.L1.py	100	78	4680
Pd.L2	100	47	2820
Pd.L2.acn	100	66	3960
Pd.L2.py	50	50	3000
Pd.L2.py	60	57	3420
Pd.L2.py	70	62	3720
Pd.L2.py	80	75	3800
Pd.L2.py	100	84	5040
Pd.L4.w	100	67	4020
Pd.L4.acn	100	76	4560
Pd.L4.py	100	77	4620

Reaction conditions: H₂O (4 mL), K₂CO₃ (1.0 mmol), time (5 min reflux), oil bath temperature (100 °C), (4-bromophenyl)methanol (1.0 mmol), benzeneboronic acid (1.2 mmol). Catalysts system: *in situ*, Pd(OAc)₂ (0.2 mol%) + ligand (0.4 mol%) or precatalyst (0.2 mol %). Yield was determined by ¹H NMR and reported to the nearest whole number.

Reaction conditions: H₂O (4 mL), K₂CO₃ (1.0 mmol), time (5 min reflux), oil bath temperature (100 °C), (4-bromophenyl)methanol (1.0 mmol), benzeneboronic acid (1.2 mmol). Catalysts system: *in situ*, Pd(OAc)₂ (0.2 mol%) + ligand (0.4 mol%) or precatalyst (0.2 mol %). Yield was determined by ¹H NMR and reported to the nearest whole number.

methylene signals [57].

3. Results and discussion

3.1. Syntheses and characterization of ligands and complexes

The ligand series **L1** – **L4** were obtained by beginning with oxidation of *o*-phenylenediamine into 2,2'-diaminoazobenzene

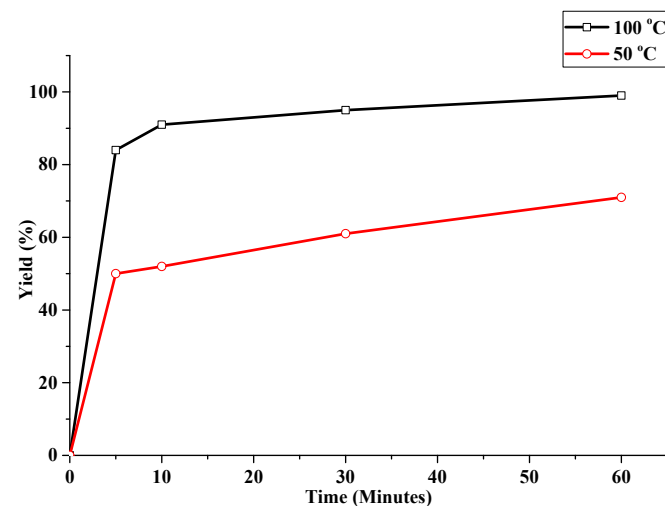


Fig. 4. Catalytic time profile of precatalyst **Pd.L2.py** at low and high temperatures (Reaction conditions: H₂O (4 mL), K₂CO₃ (1.0 mmol), time (5–60 min reflux), oil bath temperature (50 or 100 °C), (4-bromophenyl)methanol (1.0 mmol), benzeneboronic acid (1.2 mmol), **Pd.L2.py** (0.2 mol %)).

(DAB), which was then condensed with various sulfonyl chlorides using pyridine as base as well as solvent (Scheme 2). Elemental analyses and spectroscopic data gave good agreement with the identity of the ligands. Presence of solvent adducts were not found in the compounds as revealed by characterization analysis and molecular structure of compound **L1** (Fig. 1). Compound **L3** with only one sulfonyl group was isolated in addition to the targeted compound **L4**.

The palladium(II) complexes were generally obtained in good yields by stirring palladium(II) acetate and the ligand in suitable solvent at room temperature or by allowing the salt and ligand to stand in given solvents (Scheme 3). Defined coordination products were obtained for ligands **L1**, **L2** and **L4**, which generally stabilized palladium(II) as tridentate supports. Complexation experiments

with ligand **L3** were unsuccessful. Various neutral monodentate donor (**D**) species such as water, acetonitrile and pyridine occupied the fourth coordination position except for **Pd.L2**, where ligand **L2** provided the fourth coordination donor from the sulfonyl oxygen accompanied by significant distortion around the square plane of the palladium center. All the complexes were isolated as brown or purple powders/crystals.

3.2. X-ray characterization

Single crystals of **L1** and **Pd.L2.py** were obtained by slow evaporation of their acetonitrile solutions while suitable crystals of **Pd.L2.acn** and **Pd.L4.acn** were grown by slow diffusion of diethyl ether into their acetonitrile solution. **Pd.L2** was also crystalized

Table 5

Yields from various substrates with **Pd.L2.py** as precatalyst. Reaction conditions: H₂O (4 mL), K₂CO₃ (1.0 mmol), time (5 min reflux), oil bath temperature (100 °C), (4-bromophenyl)methanol (1.0 mmol), (benzeneboronic acid (1.2 mmol), preformed complex (0.2 mol %). Yield was determined by ¹H NMR and reported to the nearest whole number. *Yield recorded after 12 h.

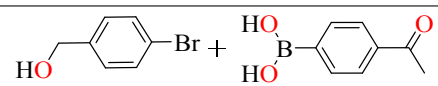
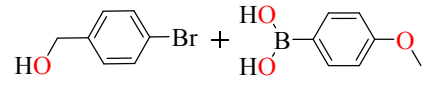
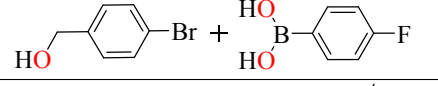
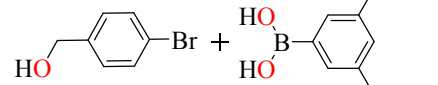
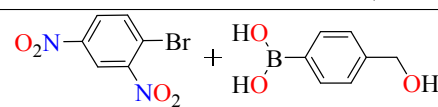
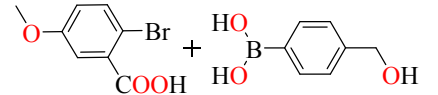
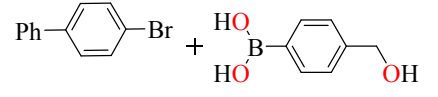
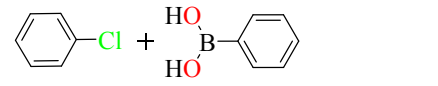
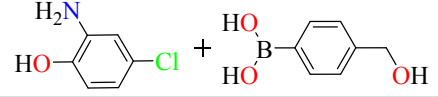
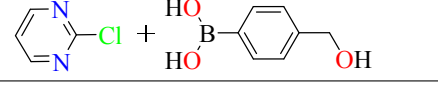
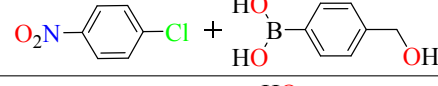
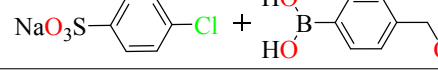
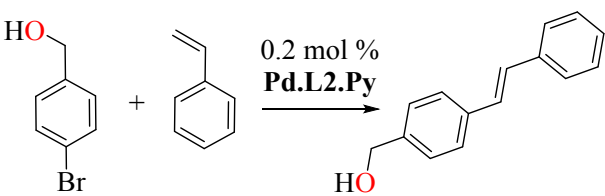
Substrates	Yield (%)	TOF (h ⁻¹)
	61	3660
	55	3300
	88	5280
	75	4500
	13	780
	26	1560
	32	1920
	trace*	
	36*	
	trace*	
	31*	
	19*	

Table 6
Testing of different reaction parameters on Heck C – C coupling



Solvent	Base	Temp. (°C) ^a	Time (hr)	Yield (%)
CH ₃ CN/H ₂ O (1:1)	K ₂ CO ₃	100	1	28
CH ₃ CN/H ₂ O (1:1)	K ₃ PO ₄	100	1	13
CH ₃ CN/H ₂ O (1:1)	Na ₂ CO ₃	100	1	17
CH ₃ CN/H ₂ O (1:1)	NaOH	100	1	8
CH ₃ CN/H ₂ O (1:1)	(NH ₄) ₂ CO ₃	100	1	6
CH ₃ CN/H ₂ O (1:1)	Cs ₂ CO ₃	100	1	Trace
DMF/H ₂ O (3:1)	K ₂ CO ₃	140	1	40
DMF/H ₂ O (3:1)	K ₂ CO ₃	140	6	74
EtOH	K ₂ CO ₃	80	1	12
EtOH/H ₂ O (3:1)	K ₂ CO ₃	100	1	8
Toluene	K ₂ CO ₃	120	1	10
Water	K ₂ CO ₃	100	"	16
Acetonitrile	K ₂ CO ₃	80	"	12

^a Temperatures presented are thermostated oil bath temperatures. Reaction conditions: Solvent: (4 mL), base (1.5 mmol), (4-bromophenyl)methanol (1.0 mmol), styrene (1.5 mmol), preformed complex (0.2 mol %). Yield was determined by ¹H NMR and reported to the nearest whole number.

by slow diffusion of n-hexane layered over its chloroform solution while suitable crystals of **Pd.L4.py** were obtained by slow evaporation of its recrystallization filtrate in acetonitrile. Structural refinement data and processing parameters were collected in **Table 1** and their Ortep plots are presented in **Figs. 1–3**.

Crystal structures of the complexes revealed tridentate N⁺N⁺N ligand chelation to the palladium center through one N-azo and two sulfonamide-substituted amine N-atoms such that one five-membered and one six-membered chelate rings occur in each of the complexes. Each complex exhibits a distorted square planar geometry around the palladium(II) metal center and bear a neutral co-ligand N- or O-donor (**D**) in the fourth coordination position except for **Pd.L2** (**Figs. 2 and 3**). Bond lengths around the coordination environment for the structures of **Pd.L2**, **Pd.L2.acn**, **Pd.L2.py**, **Pd.L4.acn** and **Pd.L4.py**, which are summarized in **Table 2**, are within expected values [58] while the azo (–N=N–) bond length of 1.264 Å in **L1** also fall within the normal range [55,59]. The shorter bond lengths between all the N-azo donors and the palladium(II) centers observed in all analyzed crystals (i.e. **Table 2**; Pd–N3 for **Pd.L2**, **Pd.L2.acn** and **Pd.L4.py**; Pd1–N2 for **Pd.L2.py** and **Pd.L4.acn**) indicate that the azo nitrogen donors possess stronger donor strengths than the sulfonyl-substituted nitrogen donors. This observation is attributable to the electron-withdrawing influence of the sulfonyl-substituents.

It could be observed that the bond lengths between the flanking sulfonamide-substituted N-donors and the metal center is generally not sensitive to steric difference between acetonitrile and pyridine co-ligands. Adding the two bonds for **Pd.L2.acn** gives ≈ 4.047 while same addition for **Pd.L2.py** gives ≈ 4.055. On the other hand, adding the two bonds for **Pd.L4.acn** gives ≈ 4.067 while same addition for **Pd.L4.py** gives ≈ 4.055, which indicates that the N-donors of the sulfonamides are slightly closer to palladium in the pyridine substituted analogue than when acetonitrile is coordinated (**Table 2**). Therefore, difference between acetonitrile- and pyridyl-coordinated counterparts could be more electronic in nature and such functional difference in the coordination sphere of

the palladium may play important roles in the ease of stable active site generation.

3.3. Determining suitable Suzuki-Miyaura coupling reaction settings

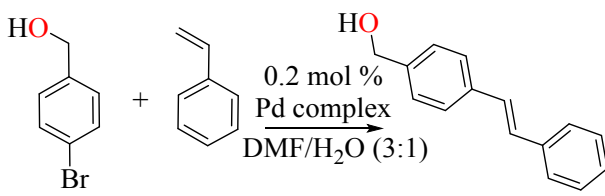
Using **Pd.L2.acn** as precatalyst (0.2 mol%), 10 min reflux duration and thermostated oil bath temperature of 100 °C, the yields of coupling (4-bromophenyl)methanol (1.0 mmol) and benzenboronic acid (1.2 mmol) were compared in the presence of 1 mmol each of K₂CO₃ and K₃PO₄ as well as in the presence of 4 mL each of water and ethanol/water mixture (3:1). **Table 3** shows that the phosphate salt did not offer advantage over the carbonate and that using only water or a mixture of water/ethanol mixture yielded no tangible difference. Therefore, further comparison of catalyst systems via *in situ* 'ligand + Pd(OAc)₂' or the comparison of preformed complexes were carried out using K₂CO₃ (1 mmol) in the eco-friendly water (4 mL). Since very high yields were already recorded at 10 min, 5 min reflux was utilized in further experiments. The other parameters remained unchanged: 0.2 mol % palladium loading, 1.0 mmol aryl bromide, 1.2 mmol boronic acid and oil bath temperature of 100 °C.

3.4. Effect of coordination environments on Suzuki coupling (by *in situ* or precatalysts)

Using water (4 mL), K₂CO₃ (1.0 mmol), '0.2 mol % Pd(OAc)₂ + 0.4 mol % ligand', oil bath temperature of 100 °C and 5 min' reflux duration, the results of *in situ* catalysis, which is presented in **Table 4**, generally showed that increasing bulkiness of the sulfonyl-substituents correlates with increasing catalyst performance (i.e. yields followed the trend **L1** (5%) < **L2** (23%) < **L3** (54%) < **L4** (63%). Therefore, it could be concluded that the ability of the ligands to form strong and stable chelate decreases from ligand **L1** to **L4**. In fact, ligands **L1**, **L2** and **L3** appear to chelate *in situ* in such a manner that limits the availability of palladium active centers when their yields are compared with the yield for coupling in the presence of Pd(OAc)₂ alone.

The precatalysts generally performed better than the corresponding *in situ* approach. However, a similar trend of ligand

Table 7
Catalytic performance of prepared complexes on Heck C – C coupling



Catalyst	Yield (%)	TOF (h ⁻¹)
Pd.L1.w	27	45
Pd.L1.acn	41	68
Pd.L1.py	29	48
Pd.L2	24	40
Pd.L2.acn	84	139
Pd.L2.py	48	80
Pd.L4.w	55	92
Pd.L4.acn	72	120
Pd.L4.py	20	33

Reaction conditions: DMF/H₂O (3 mL: 1 mL), K₂CO₃ (1.5 mmol), time (3 h reflux) oil bath temperature (140 °C), (1.5 mmol), (4-bromophenyl)methanol (1.0 mmol), styrene (1.5 mmol), preformed complex (0.2 mol %). Yield was determined by ¹H NMR and reported to the nearest whole number.

influence was observed for the precatalysts as in the *in situ* catalyst generation. The complexes bearing the methyl-substituted **L1** displayed poorer catalyst efficiency than complexes bearing the bulkier aromatic substituents (Table 4).

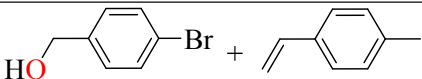
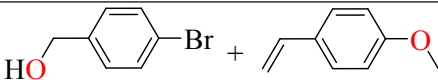
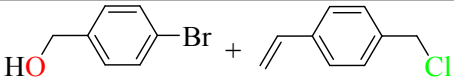
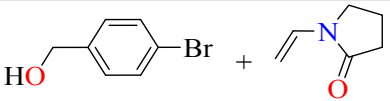
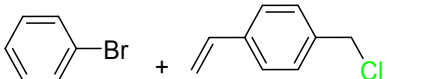
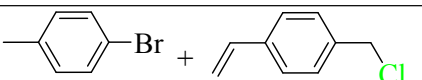
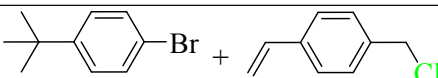
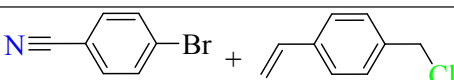
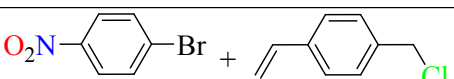
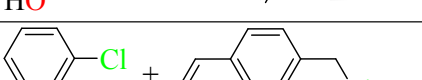
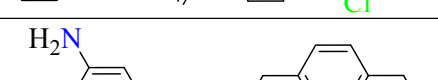
Considering the influence of the co-ligand for complexes of **L1**, **L2** and **L4**, it is noteworthy that the catalytic productivity follows the trend pyridyl > acetonitrile > water. The pyridyl-complemented complexes all performed better than their corresponding analogues and even its presence in **Pd.L1.py** made a tremendous difference to transform yields from 3% for **Pd.L1.w** and 7% for **Pd.L1.acn** to 78% for **Pd.L1.py**. The high turnover frequency (TOF) values of 4560 h⁻¹ for **Pd.L1.py**, 5040 h⁻¹ for **Pd.L2.py** and 4620 h⁻¹ for **Pd.L4.py** (420 h⁻¹) highlight the importance of the bulkier pyridyl as co-ligand. In general, it could be concluded that, the greater steric crowding of

the palladium coordination sphere by the studied ligand backbones, the more favoured the palladium catalysts is. The difference observed between **Pd.L2** (yield = 47%) without co-ligand and **Pd.L2.acn** (yield = 66%) in which acetonitrile is present as co-ligand also supports the importance of bulkier co-ligands towards catalyst improvement. Such steric demands probably create an easy route for the decomposition of the catalyst towards the formation of the active specie. [60].

Using **Pd.L2.py**, substantial activity was recorded at 50 °C, which increased with increasing temperature (Fig. 4, Table 4). Furthermore, increasing time at 50 °C and 100 °C also showed a very high initial rate as well as living catalyst behaviour.

Table 8

Other substrates in the Heck coupling. Reaction conditions: DMF/water (3:1), K₂CO₃ (1.5 mmol), time (3 h reflux), oil bath temperature (140 °C), aryl halide (1.0 mmol), olefin (1.5 mmol), preformed complex (0.2 mol %). Yield was determined by ¹H NMR and reported to the nearest whole number. *Yield recorded after 12 h.

Substrates	Yield (%)
	30
	35
	66
	22
	47
	53
	54
	44
	42
	41*
	43*
	42*
	44*

3.5. Study of substrate scope using Pd.L2.py as precatalyst

The precatalyst **Pd.L2.py** was deployed towards sterically and electronically varied substrates under the developed reaction conditions and the results are presented in Table 5. The catalytic results showed that pre-catalyst generally displayed functional group tolerance. These results are generally attractive considering the short reflux time of 5 min in the ecofriendly solvent (water). Selected aryl chlorides were also tested and products in lower yields were obtained especially for activated aryl chloride.

3.6. Determining suitable Heck coupling reaction settings

Complex **Pd.L2.py** (0.2 mol %) was used to test for suitable reaction time, solvent mixture/ratio, reaction temperature and base additive in the coupling of (4-bromophenyl)methanol and styrene as a typical Heck coupling reaction. Due to volatility, 1.5 mmol equivalent of styrene relative to (4-bromophenyl)methanol was used and reactions were typically refluxed for 1 h. The results, which are summarized in Table 6, shows that K_2CO_3 supports the Heck coupling better than K_3PO_4 , Na_2CO_3 , NaOH, $(NH_4)_2CO_3$ and Cs_2CO_3 . Furthermore, the test of solvent media revealed that dimethylformamide/water mixture (3:1), which enabled access to the higher temperature of 140 °C, is preferable for higher yield. Further reflux until 6 h in the dimethylformamide/water mixture produced 74% yield, which shows that the generated palladium active species is stable and living. Consequently, it was decided to conduct further reactions in dimethylformamide/water (3:1) at 140 °C reflux. Increasing the amount of K_2CO_3 and styrene to 2.0 mmol did not produce any significant improvement over use of 1.5 mmol of both reaction components. Therefore, 1.5 mmol of K_2CO_3 and styrene were used for further reactions; i.e. DMF/H₂O (3 mL:1 mL), K_2CO_3 (1.5 mmol), aryl bromide (1.0 mmol) and olefin (1.5 mmol) at oil bath temperature of 140 °C for 3 h' reflux time.

3.7. Effect of precatalysts coordination environments on Heck coupling

Table 7 presents the Heck coupling performance for the palladium precatalysts according to the selected reaction conditions. It could also be established that the bulkiness of the *o*-sulfonamide-azo ligands correlated with catalytic performance of the complexes. Similar to the observation in Suzuki coupling, the better catalytic results were obtained from complexes with tolyl- and 2,4,6-triisopropylphenyl-substituted ligands relative to their less bulky methyl analogues (Table 7, complexes of **L2** and **L4** compared to **L1**). However, contrary to the trend of co-ligand size observed in Suzuki coupling, pyridyl complemented coordination environments consistently yielded clearly poorer catalyst performances. Rather, the acetonitrile complemented complexes produced the highest yields among the various complexes of each ligand (see Table 7, **Pd.L1.acn**, **Pd.L2.acn** and **Pd.L4.acn**). In general, achieving a yield of 84% for complex Pd.L2.acn within 3 h of reflux under normal atmospheric condition is very encouraging because such catalytic performance is very rare within shorter reaction time. Furthermore, it could be concluded that influence of co-ligand sizes may differ for Suzuki and Heck reaction. Yields for Heck coupling of some selected aryl halide and olefin substrates catalyzed by **Pd.L2.acn** (0.2 mol %) according to the established catalytic settings above are presented in Table 8. The results generally show substrate functional group tolerance.

4. Conclusion

Ligands **L1** – **L4** and palladium complex pre-catalysts of these ligands were successfully prepared with different co-ligands in the fourth coordination position. Identities of the synthesized compounds were confirmed by single crystal structures of representative ligand and complex analogues. Within 5 min' reflux in water during *in situ* catalyst generation, higher TOF values were obtained for Suzuki couplings in the presence of palladium species bearing the bulkier triisopropylphenyl-substituted ligand **L4** while the less bulky methyl-substituted ligand **L1** behaved as poison to palladium. Similarly, the results of Suzuki couplings for the preformed complexes showed higher catalyst activities with functional group tolerance for precatalysts stabilized by ligands possessing bulkier sulfonyl substituents. High yields of 84% and 77% were obtained for the tolyl-substituted **Pd.L2.py** and 2,4,6-triisopropylphenyl-substituted **Pd.L4.py** respectively. The complexes also displayed appreciable coupling activities for Heck coupling with functional group tolerance in varying substrates.

An interesting trend observed in this study is that, while Suzuki coupling activity increased with increase in co-ligand sizes of the preformed complexes (i.e. water < acetonitrile < pyridine), the pyridyl co-ligand turned out to be very unfavourable for Heck coupling in which the best catalyst performances resulted from the acetonitrile-complemented complexes. Therefore, it could be concluded that the best catalyst setting for Suzuki coupling may not be the best for Heck reaction. Considering the fact that these Suzuki couplings were carried out within 5 min' reflux with low catalyst loading (0.2 mol %) in water, it could also be concluded that these catalysis results are generally attractive since it is often taken for granted that a strongly chelating tridentate ligands would not support active site generation.

Acknowledgements

HOO is grateful to the Government of the Federal Republic of Nigeria for financial support through TET fund research grants (TET fund AST&D year 2012 intervention) and to Adeyemi College of Education, Ondo, Nigeria for granting study leave. AOE is thankful to Alexander von Humboldt Foundation for granting post-doctoral scholarship. The DFG grants PL 155/11, PL 155/12 and PL155/13 are thankfully acknowledged.

References

- [1] H. Veisi, P. Safarimehr, S. Hemmati, Buchwald-Hartwig C-N cross coupling reactions catalyzed by palladium nanoparticles immobilized on thio modified-multi walled carbon nanotubes as heterogeneous and recyclable nanocatalyst, *Mater. Sci. Eng. C* 96 (2019) 310–318.
- [2] P. Ruiz-Castillo, S.L. Buchwald, Applications of palladium-catalyzed C-N cross-coupling reactions, *Chem. Rev.* 116 (2016) 12564–12649.
- [3] J.-B. Hong, J.P. Davidson, Q. Jin, G.R. Lee, M. Matchett, E. O'Brien, M. Welch, B. Bingenheimer, K. Sarma, Development of a scalable synthesis of a bruton's tyrosine kinase inhibitor via C–N and C–C bond couplings as an end game strategy, *Org. Process Res. Dev.* 18 (2014) 228–238.
- [4] X. Wang, M. Liu, L. Xu, Q. Wang, J. Chen, J. Ding, H. Wu, Palladium-catalyzed addition of potassium aryltrifluoroborates to aliphatic nitriles: synthesis of alkyl aryl ketones, diketone compounds, and 2-arylbzobfurans, *J. Mol. Catal. A Chem.* 78 (2013) 5273–5281.
- [5] J.R. DeBergh, N. Niljianskul, S.L. Buchwald, Synthesis of aryl sulfonamides via palladium-catalyzed chlorosulfonylation of arylboronic acids, *J. Am. Chem. Soc.* 135 (2013) 10638–10641.
- [6] A.K. Leone, E.A. Mueller, A.J. McNeil, The history of palladium-catalyzed cross-couplings should inspire the future of catalyst-transfer polymerization, *J. Am. Chem. Soc.* 140 (2018) 15126–15139.
- [7] V. Iovine, I. Benni, R. Sabia, I. D'Acquarica, G. Fabrizi, B. Botta, A. Calcaterra, Total synthesis of (±)-Kuwanol E, *J. Nat. Prod.* 79 (2016) 2495–2503.
- [8] H. Veisi, J. Gholami, H. Ueda, P. Mohammadi, M. Noroozi, Magnetically palladium catalyst stabilized by diaminoglyoxime-functionalized magnetic Fe 3 O 4 nanoparticles as active and reusable catalyst for Suzuki coupling reactions, *J. Mol. Catal. A Chem.* 396 (2015) 216–223.

- [9] H. Veisi, M. Ghorbani, S. Hemmati, Sonochemical in situ immobilization of Pd nanoparticles on green tea extract coated Fe₃O₄ nanoparticles: an efficient and magnetically recyclable nanocatalyst for synthesis of biphenyl compounds under ultrasound irradiations, *Mater. Sci. Eng. C* 98 (2019) 584–593.
- [10] S. Hemmati, L. Mehrazin, M. Pirhayati, H. Veisi, Immobilization of palladium nanoparticles on Metformin-functionalized graphene oxide as a heterogeneous and recyclable nanocatalyst for Suzuki coupling reactions and reduction of 4-nitrophenol, *Polyhedron* 158 (2019) 414–422.
- [11] M. Pirhayati, H. Veisi, A. Kakanejadifard, Palladium stabilized by 3,4-dihydropyridine-functionalized magnetic Fe₃O₄ nanoparticles as a reusable and efficient heterogeneous catalyst for Suzuki reactions, *RSC Adv.* 6 (2016) 27252–27259.
- [12] H. Veisi, A. Amini Manesh, N. Eivazi, A.R. Faraji, Palladium nanoparticles supported on 1,3-dicyclohexylguanidine functionalized mesoporous silica SBA-15 as highly active and reusable catalyst for the Suzuki–Miyaura cross-coupling reaction, *RSC Adv.* 5 (2015) 20098–20107.
- [13] H. Veisi, S.A. Mirshokraie, H. Ahmadian, Synthesis of biaryls using palladium nanoparticles immobilized on metformine-functionalized polystyrene resin as a reusable and efficient nanocatalyst, *Int.L J. Biol. Macromol.* 108 (2018) 419–425.
- [14] H. Veisi, S. Najafi, S. Hemmati, Pd(II)/Pd(0) anchored to magnetic nanoparticles (Fe₃O₄) modified with biguanidine-chitosan polymer as a novel nanocatalyst for Suzuki–Miyaura coupling reactions, *Int.L J. Biol. Macromol.* 113 (2018) 186–194.
- [15] R. Ghorbani-Vaghei, S. Hemmati, H. Veisi, An in situ generated CuI/metformin complex as a novel and efficient catalyst for C–N and C–O cross-coupling reactions, *Tetrahedron Lett.* 54 (2013) 7095–7099.
- [16] H. Veisi, M. Pirhayati, A. Kakanejadifard, Immobilization of palladium nanoparticles on ionic liquid-triethylammonium chloride functionalized magnetic nanoparticles: as a magnetically separable, stable and recyclable catalyst for Suzuki–Miyaura cross-coupling reactions, *Tetrahedron Lett.* 58 (2017) 4269–4276.
- [17] G.-P. Lu, K.R. Voigttritter, C. Cai, B.H. Lipshutz, Ligand effects on the stereochemical outcome of Suzuki–Miyaura couplings, *J. Org. Chem.* 77 (2012) 3700–3703.
- [18] M.E. Hanhan, Ligand effects in palladium-catalyzed Suzuki and Heck coupling reactions, *Appl. Organomet. Chem.* 22 (2008) 270–275.
- [19] A.R. Hajipour, A.R. Sadeghi, Z. Khorsandi, Pd nanoparticles immobilized on magnetic chitosan as a novel reusable catalyst for green Heck and Suzuki cross-coupling reaction: in water at room temperature, *Appl. Organomet. Chem.* 32 (2018) e4112.
- [20] S. Layek, Anuradha, B. Agrahari, D.D. Pathak, Synthesis and characterization of a new Pd(II)-Schiff base complex [Pd(APD)₂]: an efficient and recyclable catalyst for Heck–Mizoroki and Suzuki–Miyaura reactions, *J. Organomet. Chem.* 846 (2017) 105–112.
- [21] P. Veerakumar, P. Thanasekaran, K.-L. Lu, K.-C. Lin, S. Rajagopal, Computational studies of versatile heterogeneous palladium-catalyzed Suzuki, Heck, and Sonogashira coupling reactions, *ACS Sustain. Chem. Eng.* 5 (2017) 8475–8490.
- [22] N.D. Patel, J.D. Sieber, S. Tcyrulnikov, B.J. Simmons, D. Rivalti, K. Duvvuri, Y. Zhang, D.A. Gao, K.R. Fandrick, N. Haddad, K.S. Lao, H.P.R. Mangunuru, S. Biswas, B. Qu, N. Grinberg, S. Pennino, H. Lee, J.J. Song, B.F. Gupton, N.K. Garg, M.C. Kozlowski, C.H. Senanayake, Computationally assisted mechanistic investigation and development of Pd-catalyzed asymmetric Suzuki–Miyaura and Negishi cross-coupling reactions for tetra-ortho-substituted biaryl synthesis, *ACS Catal.* 8 (2018) 10190–10209.
- [23] H. Li, C.C.C. Johansson Seechurn, T.J. Colacot, Development of preformed Pd catalysts for cross-coupling reactions, beyond the 2010 Nobel prize, *ACS Catal.* 2 (2012) 1147–1164.
- [24] P.R. Melvin, N. Hazari, M.M. Beromi, H.P. Shah, M.J. Williams, Pd-catalyzed Suzuki–Miyaura and Miyama–Denmark couplings of aryl sulfamates, *Org. Lett.* 18 (2016) 5784–5787.
- [25] D. Sasidharan, C.V. Aji, P. Mathew, 1,2,3-Triazolylidene palladium complex with triazole ligand: synthesis, characterization and application in Suzuki–Miyaura coupling reaction in water, *Polyhedron* 157 (2019) 335–340.
- [26] X. Zhou, X. Guo, F. Jian, G. Wei, Highly efficient method for Suzuki reactions in aqueous media, *ACS Sustain. Chem. Eng.* 3 (2018) 4418–4422.
- [27] G. Meng, M. Szostak, General olefin synthesis by the palladium-catalyzed Heck reaction of amides: sterically controlled chemoselective N–C activation, *Angew. Chem.* 54 (2015) 14518–14522.
- [28] X. Cong, H. Tang, C. Wu, X. Zeng, Role of mono-N-protected amino acid ligands in palladium(II)-Catalyzed dehydrogenative Heck reactions of electron-deficient (Hetero)arenes: experimental and computational studies, *Organometallics* 32 (2013) 6565–6575.
- [29] M. Koy, F. Sandfort, A. Tlahuext-Aca, L. Quach, C.G. Daniliuc, F. Glorius, Palladium-catalyzed decarboxylative Heck-type coupling of activated aliphatic carboxylic acids enabled by visible light, *Chem. (Weinheim an der Bergstrasse, Germany)* 24 (2018) 4552–4555.
- [30] F. Christoffel, T.R. Ward, Palladium-catalyzed Heck cross-coupling reactions in water: a comprehensive review, *Catal. Lett.* 148 (2018) 489–511.
- [31] E. Jung, K. Park, J. Kim, H.-T. Jung, I.-K. Oh, S. Lee, Palladium-catalyzed Mizoroki–Heck coupling reactions using sterically bulky phosphite ligand, *Inorg. Chem. Commun.* 13 (2010) 1329–1331.
- [32] D. Roy, Y. Uozumi, Recent advances in palladium-catalyzed cross-coupling reactions at ppm to ppb molar catalyst loadings, *Adv. Synth. Catal.* 360 (2018) 602–625.
- [33] N.C. Bruno, M.T. Tudge, S.L. Buchwald, Design and preparation of new palladium precatalysts for C–C and C–N cross-coupling reactions, *Chem. Sci.* 4 (2013) 916–920.
- [34] A. Ratnam, M. Bala, R. Kumar, U.P. Singh, K. Ghosh, Design and syntheses of a new family of palladium complexes derived from tridentate ligands and their application as catalysts for Suzuki–Miyaura cross-coupling reactions, *J. Organomet. Chem.* 856 (2018) 41–49.
- [35] B. Agrahari, S. Layek, Anuradha, R. Ganguly, D.D. Pathak, Synthesis, crystal structures, and application of two new pincer type palladium(II)-Schiff base complexes in C–C cross-coupling reactions, *Inorg. Chim. Acta* 471 (2018) 345–354.
- [36] F. Saleem, G.K. Rao, A. Kumar, S. Kumar, M.P. Singh, A.K. Singh, Palladium(II) complexes bearing the 1,2,3-triazole based organosulfur/selenium ligand: synthesis, structure and applications in Heck and Suzuki–Miyaura coupling as a catalyst via palladium nanoparticles, *RSC Adv.* 4 (2014) 56102–56111.
- [37] J. Buchspies, M. Szostak, Recent advances in acyl Suzuki cross-coupling, *Catalysts* 9 (2019) 53.
- [38] S. Shi, S.P. Nolan, M. Szostak, Well-defined palladium(II)-NHC precatalysts for cross-coupling reactions of amides and esters by selective N–C/O–C cleavage, *Acc. Chem. Res.* 51 (2018) 2589–2599.
- [39] F. Schroeter, J. Soellner, T. Strassner, Cyclometalated Palladium NHC Complexes Bearing PEG Chains for Suzuki–Miyaura Cross-Coupling in Water, *Organometallics*, 2018.
- [40] T.J. Colacot, Commercial development of palladium(0) catalysts for highly selective cross-coupling reactions, *Platin. Met. Rev.* 56 (2012) 110–116.
- [41] Q.-X. Liu, Z.-L. Hu, S.-C. Yu, Z.-X. Zhao, D.-C. Wei, H.-L. Li, NHC Pd(II) and Ag(I) complexes: synthesis, structure, and catalytic activity in three types of C–C coupling reactions, *ACS Omega* 3 (2018) 4035–4047.
- [42] P. Lei, G. Meng, M. Szostak, General method for the Suzuki–Miyaura cross-coupling of amides using commercially available, air- and moisture-stable palladium/NHC (NHC = N-heterocyclic carbene) complexes, *ACS Catal.* 7 (2017) 1960–1965.
- [43] A.J. Kendall, L.N. Zakharov, D.R. Tyler, Steric and electronic influences of buchwald-type Alkyl-johnphos ligands, *Inorg. Chem. Commun.* 55 (2016) 3079–3090.
- [44] R. Firinci, M. Emin Günay, A.G. Gökçe, Synthesis, characterization and catalytic activity in Suzuki–Miyaura coupling of palladacycle complexes with n-butyl-substituted N-heterocyclic carbene ligands, *Appl. Organomet. Chem.* 32 (2018), e4109.
- [45] P. Saxena, R. Murugavel, Bulky 2,6-Dibenzhydryl-4-methylaniline derived schiff base complexes of Pd(II), Cu(II) and Co(II) as efficient catalysts for Suzuki coupling and alcohol oxidation reactions, *Chem. Select* 2 (2017) 3812–3822.
- [46] F.-M. Chen, D.-D. Lu, L.-Q. Hu, J. Huang, F.-S. Liu, Camphyl-based α -diimine palladium complexes: highly efficient precatalysts for direct arylation of thiazoles in open-air, *Org. Biomol. Chem.* 15 (2017) 5731–5736.
- [47] E. Ocansey, J. Darkwa, B.C.E. Makhubela, Synthesis, characterization and evaluation of bulky bis(pyrazolyl)palladium complexes in Suzuki–Miyaura cross-coupling reactions, *RSC Adv.* 8 (2018) 13826–13834.
- [48] L. Wang, J. Xu, H. Zhou, C. Yi, W. Xu, Cis–trans isomerization mechanism of 4-aminoazobenzene in the S0 and S1 states: a CASSCF and DFT study, *J. Mol. Catal. A Chem.* 205 (2009) 104–108.
- [49] G. Dhivya, V. Nagarajan, R. Chandiramouli, First-principles studies on switching properties of azobenzene based molecular device, *Chem. Phys. Lett.* 660 (2016) 27–32.
- [50] A.-H. Gao, B. Li, P.-Y. Zhang, J. Liu, Photochemical dynamics simulations for trans–cis photoisomerizations of azobenzene and bridged azobenzene, *Comput. Theoret. Chem.* 1031 (2014) 13–21.
- [51] S. Roy, S. Pramanik, T. Ghorui, K. Pramanik, Insight into luminescent bisazoaromatic CNN pincer palladacycle: synthesis, structure, electrochemistry and some catalytic applications in C–C coupling, *RSC Adv.* 5 (2015) 22544–22559.
- [52] J.L. Pratihari, P. Mandal, C.-H. Lin, C.-K. Lai, D. Mal, Azo-amide palladium(II) complexes: synthesis, characterization and application in C–C cross-coupling reactions, *Polyhedron* 135 (2017) 224–230.
- [53] P. Pattanayak, S.P. Parua, D. Patra, C.-K. Lai, P. Brandão, V. Felix, S. Chattopadhyay, Ruthenium and palladium complexes incorporating amino-azo-phenol ligands: synthesis, characterization, structure and reactivity, *Inorg. Chim. Acta* 429 (2015) 122–131.
- [54] J.L. Pratihari, P. Pattanayak, D. Patra, C.-H. Lin, S. Chattopadhyay, Synthesis, characterization and structure of new diazoketiminato chelates of palladium(II): potential catalyst for C–C coupling reactions, *Polyhedron* 33 (2012) 67–73.
- [55] P. Mandal, C.-H. Lin, P. Brandão, D. Mal, V. Felix, J.L. Pratihari, Synthesis, characterization, structure and catalytic activity of (NNN) tridentate azoimine nickel(II), palladium(II) and platinum(II) complexes, *Polyhedron* 106 (2016) 171–177.
- [56] R. Reuter, N. Hostettler, M. Neuburger, H.A. Wegner, Synthesis and property studies of cyclotrisazobenzenes, *Eur. J. Org. Chem.* 2009 (2009) 5647–5652.
- [57] A.O. Esolea, D. Geibig, H. Görls, W.-H. Sun, X. Hao, J.A.O. Woods, W. Plass, Palladium(II) complexes bearing 2-(1H-imidazole/oxazol-2-yl)-pyridines: synthesis, structures and ligand effects in Suzuki–Miyaura cross-coupling, *J. Organomet. Chem.* 754 (2014) 39–50.
- [58] K. Matos, L.L. de Oliveira, C. Favero, A.L. Monteiro, M. Hörner, J.-F. Carpentier, M.P. Gil, O.L. Casagrande, Palladium complexes based on tridentate pyrazolyl-

- ligands: synthesis, structures and use in Suzuki cross-coupling reactions, *Inorg. Chim. Acta* 362 (2009) 4396–4402.
- [59] J.G. Matecki, J. Nycz, Ruthenium(II) hydridecarbonyl complex with N,N'-bis(2-pyridyl)thiourea as co-ligand, *Polyhedron* 55 (2013) 49–56.
- [60] H.O. Oloyede, J.A.O. Woods, H. Görls, W. Plass, A.O. Eseola, Flexible, N-sulfonyl-substituted aliphatic amine ligands in palladium-catalyzed Suzuki-Miyaura C-C coupling: influence of substituents bulkiness and co-ligand size, *Polyhedron* 159 (2019) 182–191.